Light-based 3D printing of gelatin-based biomaterial inks to create a physiologically relevant *in vitro* fish intestinal model

Anna Szabó[1], Rolando Pasquariello[2], Pedro F. Costa[3], Radmila Pavlovic[4,7], Indi Geurs[5], Koen Dewettinck[5], Chris Vervaet[6], Tiziana A.L. Brevini[7], Fulvio Gandolfi[2], Sandra Van Vlierberghe[1*]*

Anna Szabó, author 1, Polymer Chemistry and Biomaterials Group, Centre of Macromolecular Chemistry (CMaC), Department of Organic and Macromolecular Chemistry, Ghent University, Ghent, 9000, Belgium,

E-mail: anna.szabo@ugent.be

Rolando Pasquariello, author 2, Department of Agricultural and Environmental Sciences, University of Milan, 2-20134, Italy,

E-mail: rolando.pasquariello@unimi.it

Pedro F. Costa, author 3, Biofabics Lda, Porto, Portugal

Radmila Pavlovic, author 4, Protemoics and Metabolomics Facility (ProMeFa), IRCCS San Raffaele Scientific Institute, Via Olgettina, 60, 20132, Milan, Italy

Indi Geurs, author 5, Department of Food Technology, Safety and Health, Food Structure & Function Research Group, Ghent University, Coupure Links 653, Gent 9000, Belgium

Koen Dewettinck, author 6, Department of Food Technology, Safety and Health, Food Structure & Function Research Group, Ghent University, Coupure Links 653, Gent 9000, Belgium

Chris Vervaet, author 7, Department of Pharmaceutics, Laboratory of Pharmaceutical Technology, Ghent University, Ottergemsesteenweg 460, 9000 Ghent, Belgium

Tiziana A.L. Brevini, author 8, Department of Veterinary Medicine and Animal Sciences, Laboratory of Biomedical Embryology, Università degli Studi di Milano, Via Dell'Università 6, 26900 Lodi, Italy

This article has been accepted for publication and undergone full peer review but has not been through the copyediting, typesetting, pagination and proofreading process, which may lead to differences between this version and the Version of Record. Please cite this article as doi: 10.1002/mabi.202300016.

Fulvio Gandolfi, author 9, Department of Agricultural and Environmental Sciences, University of Milan, 2-20134, Italy,

Sandra Van Vlierberghe, author 10, Polymer Chemistry and Biomaterials Group, Centre of Macromolecular Chemistry (CMaC), Department of Organic and Macromolecular Chemistry, Ghent University, Ghent, 9000, Belgium.

Email: Sandra.VanVlierberghe@ugent.be

Keywords: fish tissue engineering, hydrogel, gelatin, digital light processing

To provide prominent accessibility of fishmeal to the European population, the currently available, time- and cost-extensive feeding trials, which evaluate fish feed, should be replaced. The current paper reports on the development of a novel 3D culture platform, mimicking the microenvironment of the intestinal mucosa *in vitro*. The key requirements of the model include sufficient permeability for nutrients and medium size marker molecules (equilibrium within 24 hours), suitable mechanical properties (G' < 10 kPa), and a close morphological similarity to the intestinal architecture.

To enable processability with light-based 3D-printing, a gelatin-methacryloyl-aminoethyl-methacrylate (gel-MA-AEMA)-based biomaterial ink was developed and combined with Tween®20 as porogen to ensure sufficient permeability. To assess the permeability properties of the hydrogels, a static diffusion setup was utilized, indicating that the hydrogel constructs are permeable for a medium size marker molecule (FITC-dextran 4 kg·mol^{-1}). Moreover, the mechanical evaluation through rheology evidenced a physiologically relevant scaffold stiffness (G' = 4.83±0.78 kPa). Digital light processing (DLP)-based 3D printing of porogen-containing hydrogels resulted in the creation of constructs exhibiting a physiologically relevant microarchitecture as evidenced through cryo-scanning electron microscopy. Finally, the combination of the scaffolds with a novel Rainbow Trout (*Oncorhynchus mykiss*) intestinal epithelial cell line (RTdi-MI) evidenced scaffold biocompatibility.

1. Introduction

Due to a significant increase in the fish consumption over the past few decades, aquaculture production has struggled to meet the requirements of the global market. Therefore, the need for alternative plant- and insect-based fish feeds has become a focus of the aquaculture industry[1]. However, the effects of novel feed compositions on the fish intestinal mucosa and growth performances are currently studied via time- and cost-intensive *in vivo* feeding trials[2,3]. The development of an *in vitro* evaluation system could function as a valuable supporting strategy[4,5].

When working with farmed fish *in vitro*, the choice of fully characterized[6,7] intestinal cell lines is limited to the rainbow trout (RT, *Oncorhynchus mykiss*). At present, there only exist three available stable intestinal epithelial cell lines, being RTgutGC[8], RTdi-MI and RTpi-MI[7]. All derived cell lines are composed of a heterogenous population, retain the main properties of the tracts of origin and can form a polarized and functional epithelial barrier when cultured onto commercially available permeable membrane supports[9].

The mechanosensation[10,11] of the cell culture surface has a considerable effect on cell attachment, guidance, and differentiation. To date, these cell lines were only studied in combination with commercially available tissue culture plates (TCP) and Transwell® inserts as supports to mimic the barrier function of the cells. However, these supports are not physiologically relevant, as their stiffness is about 10^6-times higher compared to that of native intestinal tissue (E = 3 GPa[12] vs G' = 1.52 kPa[13]). Hydrogels can serve as more physiologically relevant tissue supports[14,15], as their mechanical properties are widely tailorable within a physiologically relevant range (11 Pa to 20 GPa) [16]. Aside from synthetic hydrogels, natural hydrogels, such as Matrigel® Matrix are available on the market. Matrigel® is an extracellular matrix (ECM) protein mixture with appropriate softness (34-55 Pa)[17–19], leading to superior cell attachment and differentiation compared to Transwell® inserts in combination with cancerous human intestinal cell lines, CACO2 and HT29-MTX. However, Matrigel® cannot provide the 3D shape fidelity that intestinal models require. Chemically crosslinkable hydrogels can overcome this hurdle, as upon crosslinking, the resulting hydrogel can maintain a permanent shape, which can be selected via computer-aided design[20]. During the past decades, light-based additive manufacturing techniques have emerged[21,22] and have been used in tissue engineering (TE) to create scaffolds for cell support, as they can provide a life-like mimicry to native tissue down to nanometer

scale, depending on the technique used[23]. Digital light processing (DLP) 3D printing[24,25] is an inexpensive, stereolithography-based technology, where ultraviolet (UV) or visible light is employed in combination with a projection on a digital micromirror device (DMD) to create 3D structures in a layer-by-layer fashion with acceptable resolution (0.6 µm to 90 µm)[26]. To exploit stereolithography-based 3D printing, a biomaterial ink formulation is developed, which usually consists of a photo-crosslinkable polymer, a solvent, a photoinitiator (PI) and a photoabsorber (PA)[27] .

Stereolithography-based 3D printing has already been exploited for the development of *in vitro* intestinal models, exploiting synthetic polymers, such as acrylated poly(ethylene glycol) (PEG-DA) in combination with cell-interactive compounds, such as fibronectin[28]. Alternatively, synthetic polymers, as ε-polycaprolactone, have also been combined with photo-crosslinkable gelatin derivatives, such as gelatin-methacryloyl (gel-MA)[29] to achieve cell-interactivity in combination with CACO2 cells[30]. To improve the processability of gelatin derivatives and overcoming the need for the utilization of additional crosslinkers upon 3D printing, Van Hoorick et al have developed gelatin-methacryloyl-aminoethyl-methacrylate (gel-MA-AEMA). It has not only shown superior CAD-CAM mimicry upon processing with two-photon polymerization (2PP), as compared to gel-MA as benchmark, yet also excellent biocompatibility [31]. To create a relevant intestinal epithelial model, hydrogel constructs should be sufficiently permeable. To achieve this, several methods have already been described, such as salt/porogen leaching, or cryogelation[32,33]. However, the combination of the latter strategies with 3D printing is challenging. Alternatively, surfactants (Tween®20, Span®20) can be exploited since they form micelles in aqueous solutions. They were previously applied in combination with poly(vinyl alcohol), collagen and alginate hydrogels towards wound dressing applications[34], as well as for the fabrication of porous, conductive materials via DLP 3D printing based on dipropylenglycol diacrylate, dipentaerythritol hexaacrylate and trimethylolpropane-triacrylate[35].

In the present work, we describe the development of a novel *in vitro* hydrogel-based fish intestinal model. To this end, we created a gel-MA-AEMA-based hydrogel construct containing Tween®20, as porogen to improve the permeability properties of the constructs, followed by mechanical evaluation and permeability studies with medium size marker molecules. The optimal biomaterial ink formulation has been applied in DLP 3D printing, to achieve a 3D intestinal micromorphology with cones providing a villi-like structure. Finally, the hydrogels were seeded with RTdi-MI cells to evaluate the biocompatibility of the hydrogel constructs as reflected by cell proliferation and monolayer formation.

2. Materials and methods

2.1. Biomaterial ink development

2.1.1.Materials

Gelatin type B was extracted from bovine hides by an alkaline treatment and kindly provided by Rousselot (Ghent, Belgium). Phosphate buffered saline (PBS), methacrylic anhydride, deuterium oxide (D_2O), FITC-Dextran 4 kg·mol^{-1} and Tween®20 were purchased from Sigma-Aldrich (Diegem, Belgium). Disinfectol and sodium dihydrogen phosphate ($NaH_2PO_4 \cdot 2\ H_2O$) were purchased from Chemlab (Zedelgem, Belgium). 1-ethyl-3-(3-dimethylamino)propyl)-carbodiimide hydrochloride (EDC) and Ponceau 4R were obtained from TCI Europe (Zwijndrecht, Belgium). Dimethyl sulfoxide (DMSO, 99.85%), N-hydroxysuccinimide (NHS, 98%) and sodium nitrate ($NaNO_3$) were obtained from Acros (Geel, Belgium). 2-Aminoethyl methacrylate hydrochloride (AEMA·HCl) was purchased from Polysciences (Conches, France). Dialysis membranes Spectra/Por (MWCO 12.000−14.000 g/mol) were acquired from Polylab (Antwerp, Belgium). The utilized photo-initiator, lithium 2,4,6-trimethylbenzoylphenylphosphinate (Li-TPO-L) was synthesized in-house based on a previously described procedure[36]. The L-15 media were purchased from Thermo Fisher Scientific (Merelbeke, Belgium).

2.1.2.Development of gelatin-methacryloyl-aminoethyl-methacrylate (gel-MA-AEMA)

The development of gel-MA-AEMA involved a two-step derivatization. In a first step, the methacrylation of gelatin type B was performed[37]. 100 g of gelatin B was dissolved at 40 °C under continuous stirring in 1 L phosphate buffer (pH 7.8). Subsequently, 2.5 equivalents, relative to the amount of amine groups in gelatin type B (0.0385 mol/100 g), methacrylic anhydride (14.34 mL; 96.25 mmol) were added, followed by reaction for 1 hour and dialysis for 24 hours at 40 °C against deionized water (DW, MWCO 12,000 – 14,000 Da). The pH of the solution was then adjusted to 7.3 followed by lyophilization (Christ freeze-dryer Alpha2). In the second step, the methacrylation of the carboxylic groups of gel-MA was performed [31]. 60 g gel-MA (DS: 97 %, 66 mmol carboxylic acids) was dissolved at 50 °C in 525 mL dry DMSO under inert atmosphere. After dissolution, 0.5 equivalents of EDC (6.314 g; 0.033 mol) and 0.75 equivalents of NHS (5.687 g; 0.049 mol) were added simultaneously to the mixture together with 40 mL dry DMSO under inert atmosphere. After 30 minutes, 0.5 equivalents of 2-aminoethylmethacrylate hydrochloride (AEMA·HCl) (5.456 g; 0.033 mol) and 0.01 equivalents of 4-tert-butyl catechol (0.110 g; 0.001 mol) were added to the solution, together with 40 mL dry DMSO. The reaction mixture was kept under inert atmosphere and shielded from light for 24 hours at 50 °C.

The solution was then precipitated in a 10-fold excess of acetone at room temperature, followed by filtration on a Buchner Filter (filter paper 10-12 µm pore size). Next, the precipitate was redissolved in double-distilled water (DDW), followed by 24-hour dialysis (MWCO 12.000−14.000 Da) against distilled water (DW) at 40 °C. After dialysis, the pH was set to 7.3 with NaOH solution and consequently lyophilized (Christ freeze-dryer Alpha2).

2.1.3.Physico-chemical characterization of gel-MA-AEMA

Structural analysis of hydrogel precursors via proton nuclear magnetic resonance (^{1}H-NMR) spectroscopy

To quantify the degree of substitution (DS, defined by the percentage of substituted side groups) of the developed gelatin derivatives, ^{1}H-NMR spectroscopy was performed (Bruker WH 500 MHz) in deuterated water (D_2O) at 40 °C. The integrals of the characteristic peaks of the methacrylamide moieties (5.5 ppm (s,1H) and 5.51 ppm (s, 1H)) (gel-MA and of the methacrylate moieties (6.20 ppm (s, 1H) and 5, 80 (s, 1H) (gel-MA-AEMA) were correlated to the integrals of the characteristic peak of the inert hydrogens of Val, Leu, and Ile at 1.01 ppm (18H) according to the following formulas as previously described (Equation 1 and 2) [31].

$$DS\ amines\ (\%) = \frac{\frac{I5.51\ ppm + I5.75}{2 * \frac{0.0385 mol}{100 g}}}{\frac{I1.01\ ppm}{\frac{0.3836 mol}{100 g}}} * 100 \quad (1)$$

$$DS\ carboxylic\ acids\ (\%) = \frac{\frac{I6.20\ ppm}{0.1098\ mol/_{100\ g}}}{\frac{I1.01\ ppm}{0.3836\ mol/_{100\ g}}} * 100 \quad (2)$$

Molar mass determination of hydrogel precursors via gel permeation chromatography (GPC)

The molar mass (number average, M_n and weight average, M_w), and the dispersity ($Đ$) of the hydrogel precursors were studied by GPC (Shodex™ OHpak™ SB-806M HQ columns coupled to a Waters 600 separation module followed by a Waters 410 Refractive Index detector). First, a five-point calibration curve exploiting pullulan standards (Shodex, molar mass range 6,100 - 622,000 g/mol) was established, followed by measuring the precursors. All samples were dissolved in a phosphate-nitrate buffer at a 10 mg/ml concentration and filtered with a 0.45 µm pore size membrane before injection[38].

Rheological evaluation of crosslinkability of hydrogel precursors

The crosslinking kinetics of the modified gelatins were determined using a Physica MCR-301 rheometer with parallel plate setup (upper plate diameter d = 25 mm). A 300 µL gel-MA / gel-MA-AEMA solution (10 w/v% in DDW, in the presence of 2 mol% Li-TPO-L as photoinitiator with respect to the amount of double bonds present in the material) was placed between the parallel plates of the rheometer at a 0.35 mm gap height, followed by trimming and sealing the edges with silicon grease to avoid sample drying. The samples were irradiated with 10 mW/cm^2 UV-A light (320-500 nm, EXFO Novacure 2000 UV light source) at 37 °C with a constant oscillation frequency of 1 Hz, at a strain of 0.1% and 0.5 N normal force. The storage (*G'*) and loss moduli (*G"*) were monitored as a function of time.

2.1.4.Development and characterization of a porous, gel-MA-AEMA-based hydrogel film

Film-casting of porous, gel-MA-AEMA-based hydrogels

Gel-MA-AEMA (0.375 g) was dissolved in 3 mL phosphate buffered saline (PBS, pH 7.4) at 40 °C to obtain concentrations of 15 w/v %, in the presence of 2 mol% Li-TPO-L, with respect to the amount of double bonds. To create a porous hydrogel structure, Tween®20, a non-ionic surfactant was added to the solutions in different concentrations (8-17 v/v % with respect to PBS), followed by vigorously mixing of the solutions. The solutions were kept at 40 °C for another 15 minutes and were injected between two parallel glass plates covered with a polypropylene foil, separated by a 200 µm thick silicone spacer. The solutions were irradiated with UV-A light from both sides (10 mW/cm^2, λ = 365 nm) for 30 min. To remove the porogen from the crosslinked hydrogel structures, the films were washed in 70% EtOH (Disinfectol) for 24 hours, followed by incubation in PBS at 20 °C for 24 h to obtain equilibrium swelling.

Morphological evaluation of the film-casted porous, gel-MA-AEMA-based hydrogels

To study the pore size of the porous, gel-MA-AEMA-based hydrogel constructs, scanning electron microscopy (SEM, FEI, Phenom) was used. Prior to visualization, the samples were vacuum dried at room temperature and gold sputtered (Automatic Sputter Coater K550X with a RV3 two stage rotary vane pump). The visualization was performed in backscattered electron (BSE) analysis mode.

Porosity evaluation of the porous gel-MA-AEMA-based hydrogels

The porosity of the hydrogel constructs was evaluated via He pycnometry (AccuPyc 1330, Micromeritics, Norcross, USA). The true volume of the hydrogel films was evaluated with He pycnometry. The porosity was then calculated based on the difference between the bulk and true volume of the film casted samples. Prior to the pycnometry measurements, the films were vacuum dried at room temperature. The porosity of the films was calculated exploiting Equation 3[39]:

$$Porosity\ (\%) = \frac{bulk\ volume - true\ volume}{bulk\ volume} * 100 \quad (3)$$

Mechanical evaluation of the film-casted porous, gel-MA-AEMA-based hydrogels

A Physica MCR-301 rheometer with parallel plate setup (upper plate diameter d = 15 mm) was exploited. The equilibrium swollen 200 µm thick hydrogel samples were punched out (d = 14 mm) and placed on the bottom plate of the rheometer. Subsequently, a frequency of 1 Hz and 2% constant shear amplitude were applied on the samples combined with a 0.27 N normal force during 3 minutes according to the protocol from Deptuła et al, at 20 °C, n = 5 [13]. The storage modulus (*G'*) was recorded as a function of time.

Permeability studies of the film-casted, porous gel-MA-AEMA-based hydrogels

To evaluate the permeability properties of the 200 µm thick, gel-MA-AEMA-based hydrogels, FITC-Dextran 4 kg·mol^{-1} was used as paracellular marker molecule. A previously described protocol established by Pasquariello et al was adapted [7]. The hydrogel constructs were mounted in the adjustable inserts of Biofabics®, which enabled to evaluate the permeability properties of the membranes without exploiting any additional supporting membranes, influencing the obtained values (Figure 1). Briefly, 200 µL of L-15 complete medium supplemented with 200 µM FITC-dextran (4 kg·mol^{-1}) was pipetted in the apical compartment of the inserts from Biofabics®, and 2.5 mL PBS was pipetted into the basolateral compartment. Absolute quantification of FITC-dextran 4 kg·mol^{-1} was performed after collecting 100 µL samples from both the apical and the basolateral compartments after 24 h followed by read-out using a Multimode microplate reader (Wallac 1420; EX: 490 nm; EM: 520 nm).

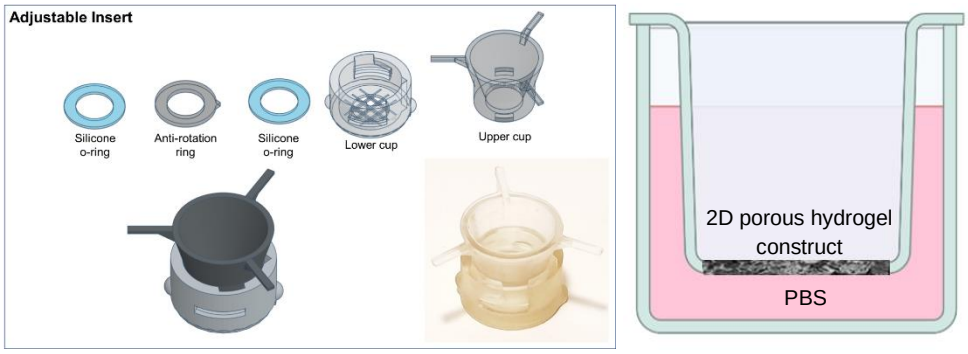

Figure 1. Schematic figure of a custom-made adjustable insert developed by Biofabics® (left) and schematic figure representing the application of the porous 2D hydrogel constructs in the insert (right).

2.1.5.Development of a porous, 3D gel-MA-AEMA-based hydrogel construct

Computer aided designing (CAD) of physiologically relevant intestinal structure

The wall of Rainbow Trout intestine lacks the crypts of Lieberkühn and the villi, which are typical intestinal elements in mammalian species. Instead, the mucosa presents folds, typically in the size range of 200-400 µm height and approximately 100 µm width at their base (referred as villi-like structures throughout the manuscript)[1]. The CAD model was designed to follow the biological morphology and to ensure compatibility with Biofabics' adjustable insert. To this end, a circular arrangement of the villi-like structures was applied with 150-200 µm spacing between the folds on a 200-350 µm thick supporting layer. The size of the villi-like structures was 425 µm in height and 200 µm in width at the bottom of the structures, decreasing to 100 µm width towards the top (apex) (Figure S2). The design was created with SolidWorks 2021.

Biomaterial ink development

The detailed experimental section regarding the optimal photoinitiator and photoabsorber content can be found in the supporting information.

In the optimized formulation, gel-MA-AEMA (0.0625 g) was dissolved in 0.5 mL phosphate buffered saline (PBS, pH 7.4) at 40 °C to obtain concentrations of 15 w/v%, in the presence of 11 mol% of Li-TPO-L as PI and 0.9 mol% of Ponceau 4R as PA, with respect to the amount of double bonds present. To create a 3D porous hydrogel structure, Tween®20, a non-ionic surfactant was added to the solutions

(8 v/v% with respect to PBS), followed by vigorous mixing of the solution. The solution was transferred to the vat of the printer (CellInk LumenX+) and the printing parameters were set at 25.1 mW/cm^2 intensity, 6.5 s curing time/layer at elevated temperature (37 °C).

Morphological evaluation of the 3D printed constructs

To visualize the 3D samples, cryo-scanning electron microscopy (cryo-SEM, JEOL JSM-7100F equipped with the cryo-transfer system Quorum PP3010T) was utilized. The samples were equilibrium swollen in PBS at 20 °C and taped on a sample holder. Subsequently, they were frozen in liquid nitrogen, followed by a sublimation cycle of 30 min at -70°C. Afterwards, they were covered in platinum and visualized with SEM (acceleration voltage 3 kV, 350x magnification).

2.2. Biocompatibility of the gel-MA-AEMA-based hydrogel constructs

2.2.1.Materials

L-15 complete medium was purchased from Thermo Fisher Scientific (Waltham, MA, USA). Phalloidin-iFluor 594 Reagent was obtained from Abcam (Cambridge, United Kindom). BCIP/NBT substrate (5-bromo-4-chloro-3-indolyl phosphate/nitroblue tetrazolium) was purchased from Vector Laboratories (Burlingame, CA, USA). L-glutamine, antibiotic/antimycotic solution, Fetal Bovine Serum (FBS), paraformaldehyde, Phosphate Buffered Saline (PBS), Bovine Serum Albumin (BSA), Triton X-100, DAPI, Tris-HCl were purchased from Sigma-Aldrich, Milan, Italy.

2.2.2.Determination of the optimal seeding density

To determine the optimal seeding density, epithelial intestinal RTdi-MI cells (passages between 45 and 50), derived by Pasquariello et al [7], were seeded at the following concentrations: 60,000, 120,000, 240,000, 500,000 and 900,000 cells/cm² on the 3D gel-MA-AEMA hydrogel constructs. The cells were then cultured in Leibovitz's complete L-15 complete medium supplemented with 2 mM L-glutamine, 10,000 units/mL penicillin, 10.0 mg/mL streptomycin, and 25.0 µg/mL amphotericin B (antibiotics) and 5% FBS and maintained at 20 °C under ambient atmosphere over the course of 24 days. L-15 complete medium was replaced twice a week. To evaluate cell confluency, the cells were stained for 4,6-diamidino-2-phenylindole (DAPI) as described below.

2.2.3. *Cell growth and morphological analysis*

Cells were fixed in paraformaldehyde (PFA) solution (4% in PBS) at room temperature for 30 min. Then, cell nuclei were stained with DAPI for 20 min at room temperature. Thereafter, the cells were washed 3 times using PBS. Images of at least 5 hydrogels of 3 different independent experiments were acquired using a ZEISS Axio Zoom.V16 microscope (ZEISS, Italy, Europe) after 3, 10, 17 and 24 days of culture. The percentage of confluence was calculated as area without cells divided by the growth area of the hydrogel membranes (0.5 cm^2). To further confirm the results of confluence, cells were stained for filamentous actin (F-actin). To this end, cells were fixed in 4% PFA in PBS. Thereafter, to prevent aspecific binding, the cells were incubated at room temperature for 30 min in a blocking buffer containing 5% BSA and 0.3% Triton X-100 in PBS. The cells were then washed 3 times using PBS and were stained for F-actin using Phalloidin-iFluor 594 Reagent. Nuclei were counterstained with DAPI. Confocal imaging was carried out using the A1R microscope (Nikon, Tokyo, Japan).

2.2.4.Evaluation of cell differentiation

Cell differentiation was evaluated analyzing intestinal alkaline phosphatase (IAP) activity, which is a marker of terminally differentiated enterocytes[7,9]. The cells were first fixed in 4% PFA for 30 min at room temperature, and thereafter, incubated with BCIP/NBT substrate (5-bromo-4-chloro-3-indolyl phosphate/nitroblue tetrazolium (Vector Laboratories, SK-4500 USA), which produces a blue reaction product in the presence of the IAP enzyme and Tris-HCl (pH = 9.3). The cells were then rinsed in PBS and counterstained using Mayer's hematoxylin. Images were acquired using ZEISS Axio Zoom.V16 microscope (ZEISS, Italy, Europe).

2.3. Statistical analysis

At least 3 replicates were used for each experiment and are presented as the mean ± standard deviation. OriginPro 2021 was utilized to perform one-way variation analysis (ANOVA) and student's t-tests, unless otherwise stated. Results were considered statistically significant if $P < 0.05$.

3. Results and discussion

3.1. Biomaterial ink development

3.1.1.Physico-chemical characterization of the hydrogel precursors

Physico-chemical characterization of the hydrogel precursors was performed to verify the modification of gelatin type B. The structural analysis performed via ^{1}H-NMR spectroscopy confirmed that 97% (0.37 mmol/100 g of gelatin) of the amine moieties of gelatin type B were converted into methacrylamide functionalities during the first modification step (Figure 2/A), which is in line with previous reports[31]. In the second step of the functionalization, carbodiimide coupling chemistry was applied for the activation of the carboxylic acid moieties of gel-MA, towards functionalizing them with 2-aminoethyl methacrylate (AEMA), as previously reported. The degree of substitution (DS), calculated using Equation 2, was 25% (0.27 mmol/100 g gelatin)[31].

To evaluate the molar mass change throughout the modification procedure, gel permeation chromatography was used. Table 1 summarizes the obtained molar mass and dispersity values for unmodified gelatin type B, the intermediate gel-MA product and gel-MA-AEMA. The results suggest that the 2-step synthesis leads to hydrolysis of the starting product, as reflected by the decrease of the molar mass, resulting from water traces present in the solvent. In addition, hydrolysis of the gelatin chains also occurs during dialysis. The results are in line with previous observations from Van Hoorick et al[31].

Table 1. Gel permeation chromatography evaluation of molar mass and dispersity of unmodified gelatin type B, gel-MA and gel-MA-AEMA.

	Number average molar mass, Mn [g/mol]	Weight average molar mass, Mw [g/mol]	Dispersity, Đ [-]
Gel type B	48900	146000	2.98
Gel-MA	22000	63000	2.87
Gel-MA-AEMA	18300	29400	1.60

In situ rheological measurements confirmed that both the intermediate gel-MA product and gel-MA-AEMA were photo-crosslinkable in the presence of 2% Li-TPO-L photoinitiator at 37 °C. *G'* of gel-MA-AEMA (4.5 ± 0.5 kPa) was lower than previously reported (14.9 ± 0.2 kPa) by Van Hoorick et al[31], which is anticipated to result from a more pronounced molar mass decrease during the second synthesis step. The duration of the second step was extended to 24 hours (instead of overnight). Consequently, more hydrolysis could occur resulting in a lower molar mass of the final product. The crosslinking kinetics confirmed that a higher amount of methacrylates led to superior crosslinking rates, which can be favorable in the context of light-based 3D printing (Figure 2/B). Higher crosslinking rates reduce the processing time of the desired structures. However, the utilization of photoabsorbers is generally favorable to gain superior control over the process (Table S1).

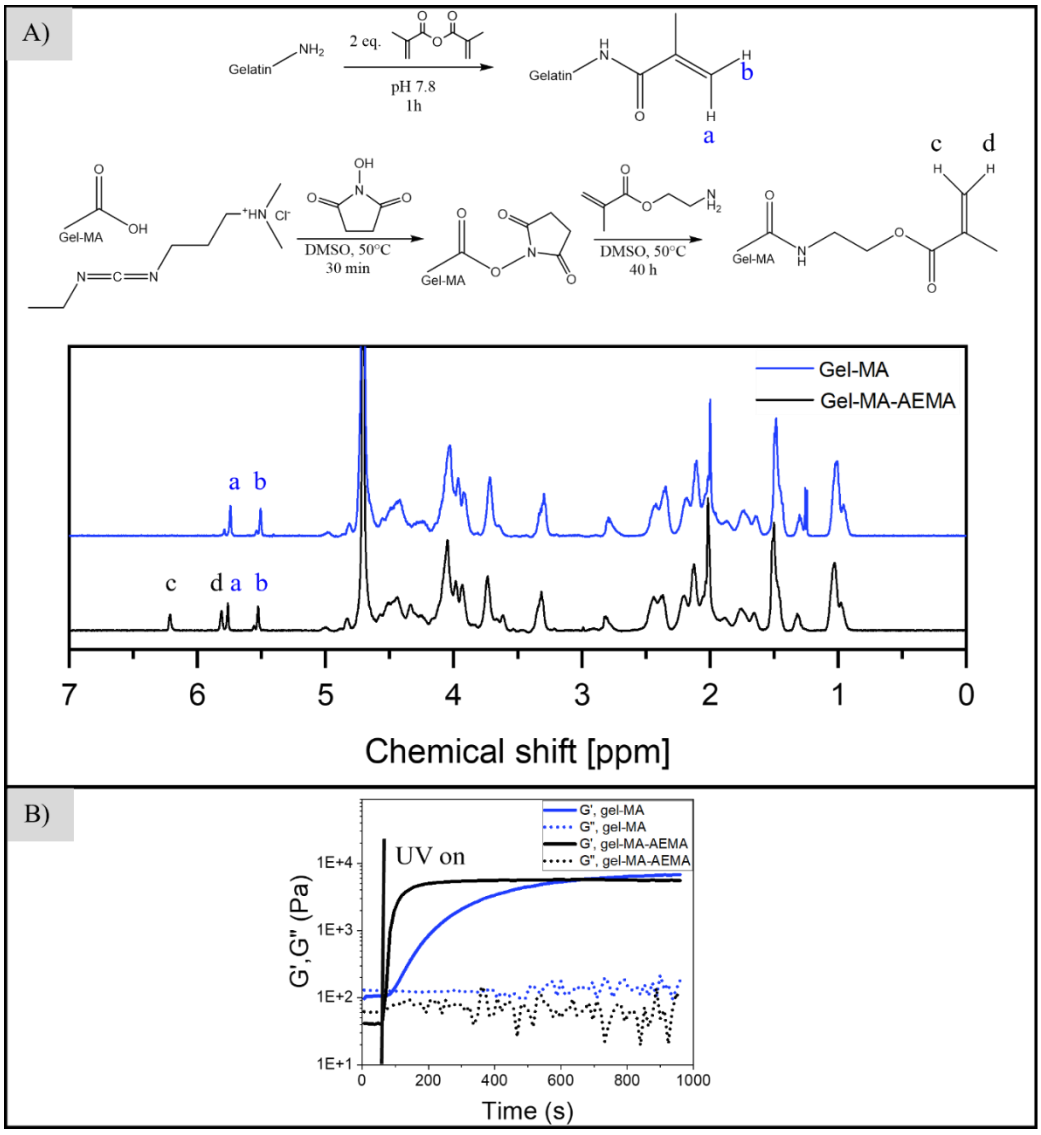

Figure 1. Physico-chemical characterization of gel-MA and gel-MA-AEMA. Figure 2/A The ^{1}H-NMR spectra evidence the presence of MA moieties as reflected by the signals at 5.51 and 5.75 ppm for gel-MA, and the additional characteristic peaks at 5.80 and 6.20 ppm for gel-MA-AEMA. Figure 2/B The *in situ* rheology data suggest superior crosslinking kinetics of gel-MA-AEMA compared to gel-MA due to the increased amount of crosslinkable moieties present.

3.1.2.Evaluation of physiological relevance of the gel-MA-AEMA-based porous hydrogel films

Morphological evaluation of the film-casted porous, gel-MA-AEMA-based hydrogels

To create a porous hydrogel structure, Tween®20, a non-ionic surfactant was incorporated in the hydrogels. The goal was to create a porous hydrogel film with a pore size in a range that does not permit infiltration of epithelial cells inside the films yet improves the permeability properties of the hydrogel constructs. To assess the optimal porogen content in combination with the hydrogel precursors, different concentrations of Tween®20 were added to the formulations prior to photo-crosslinking. The pore size distribution obtained following the washing step is shown as a function of the porogen content (v/v%) in Figure 3/B. The SEM micrographs show that the average pore size (from 11±17 µm up to 77±76 µm) and its distribution increase upon increasing the porogen content from 8 v/v% to 17 v/v%. The He pycnometry-based porosity measurements (Figure 3/C) confirmed that the overall porosity of the films increased as a function of the porogen concentration, although at 17% porogen content, a slight decrease in porosity was observed, resulting from phase separation of the Tween®20 and the hydrogel precursor solution. Hence, a concentration of 8 v/v% porogen (Figure 3/A) was selected for further studies as preliminary cell culture tests have shown that gel-MA-AEMA-based hydrogels with higher porogen contents cannot prevent penetration of RTdi-MI cells through the films.

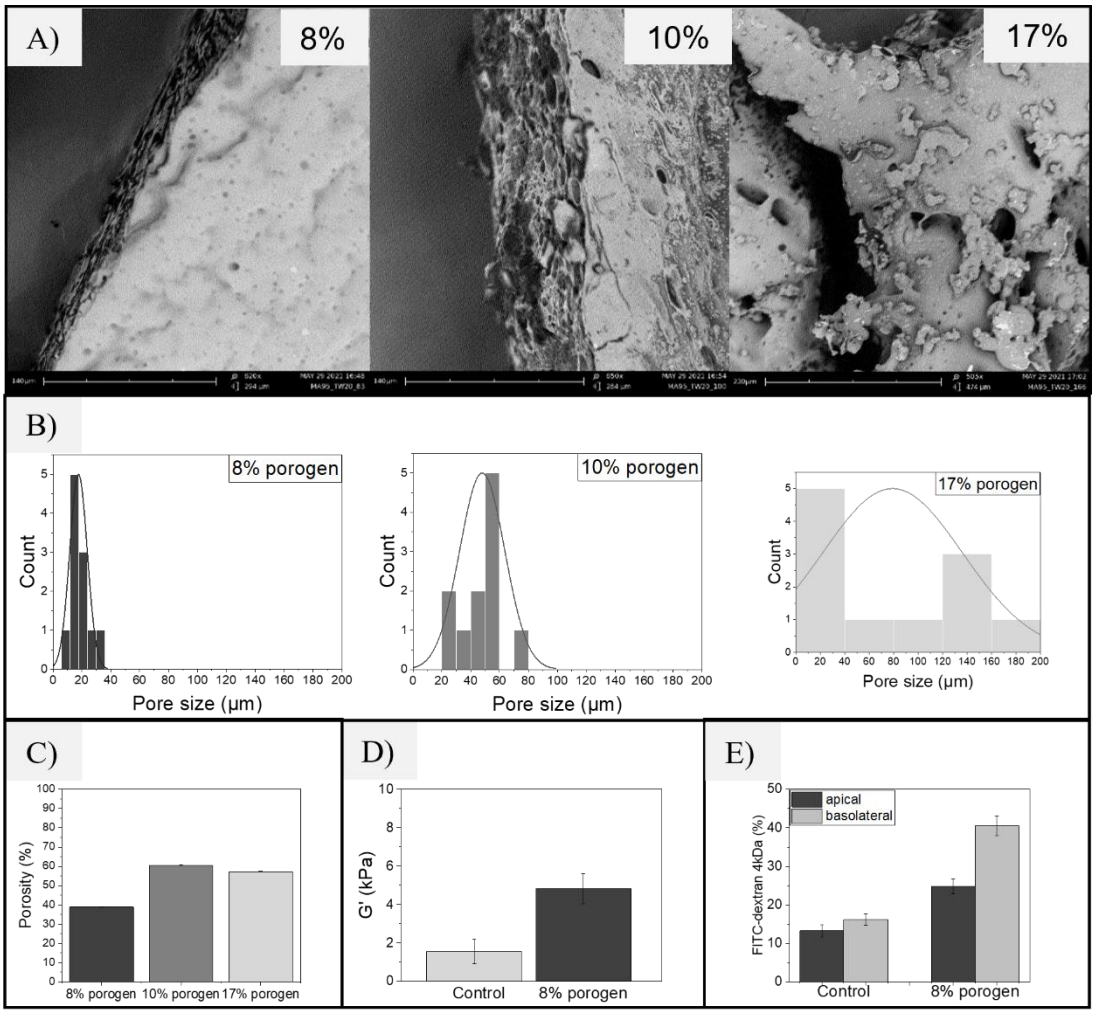

Figure 3. Characterization of the porous 2D hydrogel constructs. Figure 3/A show the optimization of the porogen (Tween®20) content within the constructs to achieve an overall porous structure. Figure 3/B shows the pore size distribution in the porous hydrogel constructs upon increasing the porogen content. Figure 3/C presents the porosity of the 2D hydrogel constructs as a function of the porogen content. Upon increasing the porogen concentration in the hydrogel precursor solutions, an enhanced porosity is achieved, although at 17% porogen content, a decrease is observed due to phase separation occurring in the system. Figure 3/D represents the mechanical properties of the non-porous and 8 v/v% porogen-containing 200 μm thick films. The oscillatory rheological evaluation confirms that the mechanical properties of the constructs are situated in the required stiffness range ($G' \leq 10$ kPa). Figure 3/E confirms the enhanced efficiency of the porous structure towards an efficient diffusion of medium size marker molecules (FITC-dextran 4 kg·mol^{-1}) through the hydrogels compared to the non-porous control hydrogel films (sample thickness 200 μm).

Mechanical evaluation of the film-casted porous, gel-MA-AEMA-based hydrogels

To assess the mechanical properties of the gel-MA-AEMA-based hydrogel films, parallel plate rheology was performed at 20 °C. The mechanical properties of the non-porous gel-MA-AEMA hydrogel films and the ones containing 8 v/v% porogen concentration with a 200 µm thickness were evaluated. According to Deptuła et al*, ex vivo* human intestinal samples are characterized by a stiffness of *G'* = 1.52 kPa in case of healthy tissue and *G'* = 9.67 kPa in case of cancerous tissue[13]. The measured values are in the line with the observation of Gjorevski et al, which suggests 1.3 kPa as ideal scaffold stiffness for intestinal stem cell (ISC) and organoid cultures[40]. However, in case of mouse ISC He et al suggests 0.6 kPa as ideal scaffold stiffness[41]. So far, no similar studies have been performed with fish intestinal samples, therefore we used these as reference values. We targeted a hydrogel construct with a stiffness close to *G'* = 1.5 kPa and lower than 10 kPa. In case of non-porous, control gel-MA-AEMA samples (0 v/v% Tween®20 content), a stiffness of 1.56 ± 0.63 kPa was obtained, while for a porous (8 v/v% Tween®20-content) hydrogel, a stiffness of *G'* = 4.83 ± 0.78 kPa was recorded, which shows that the introduction of the porous morphology causes a significant change in the stiffness of the samples[42] (Figure 3/D).

Permeability studies of the 3D printed porous gel-MA-AEMA-based hydrogels

To determine the permeability properties of the porous 2D hydrogels, the diffusion of FITC-dextran 4 kg·mol^{-1} was monitored after 24 hours. Previously, Pasquariello et al determined the diffusion properties of FITC-dextran 4 kg·mol^{-1} of commercially available Transwell® inserts without cells seeded. They showed that within 24 hours, 49.4±1.9% of the relative amount of FITC-Dextran 4 kg·mol^{-1} was retained in the apical compartment, while 50.5±2.3% was diffused to the basolateral compartment[7]. The current tests performed on the 200 µm thick, non-porous hydrogel films show 13.3±1.5% retention of the compound in the apical compartment, and a 16.2±1.6% FITC-dextran 4 kg·mol^{-1} transport to the basolateral compartment, while porous hydrogels with 8% porogen content show 24.8±2.0% retention in the apical compartment, and a more pronounced, 40.5±2.6% FITC-dextran 4 kg·mol^{-1} transport to the basolateral compartment (Figure 3/E). This indicates that gel-MA-AEMA-based hydrogels absorb a substantial amount of FITC-dextran 4 kg·mol^{-1}. However, upon introducing an overall porous structure, the permeability properties of the hydrogel constructs significantly

increase. Hence, the developed porous hydrogel construct is appropriate for the evaluation of the barrier formation of RT-di-MI cells in future work.

3.1.3.DLP 3D printability of biomaterial ink composition

The developed biomaterial ink composition showed a reproducible 3D printing capacity. Morphological analysis confirmed the appearance of villi-like structures as part of the hydrogel scaffolds. Moreover, the top view of the construct showed an even distribution of the villi-like structures, whereas the side view evidenced the shape and smoothness of the structures. The cross-section of the 3D printed construct confirms the formation of a porous structure. The obtained average villi-like structure thickness is 202±11 µm at the bottom of the constructs, while the average height is 178±7 µm (Figure 4), which ensures a close mimicry of physiological morphology[9]. Based on the initial villi-like structure size from the CAD design (Figure S2, width 200 µm, height 425 µm), the width shows a 100% CAD-CAM mimicry in the x-y dimension, combined with a 40% CAD-CAM mimicry in the z direction. Torras et al[43] previously reported DLP 3D printing of 5 w/v% gel-MA blended with 3 w/v% PEG-DA into intestine-like structures (I = 12.3 mW/cm^2, 5 s exposure time/layer). More specifically, they observed an x-y CAD-CAM mimicry of 83% (250 µm vs 300 µm CAD thickness) and a 70% z dimension CAD-CAM mimicry (700 µm vs 1000 µm height)[43]. A lower CAD-CAM mimicry in the z dimension was observed in case of the gel-MA-AEMA-based biomaterial ink, compared to the gel-MA/PEG-DA blend upon 3D printing of intestinal structures. However, the advantage of the currently developed gel-MA-AEMA-based biomaterial ink is that there is no need to include additional synthetic crosslinkable polymers in the DLP formulation to obtain physiologically relevant villi-like structures.

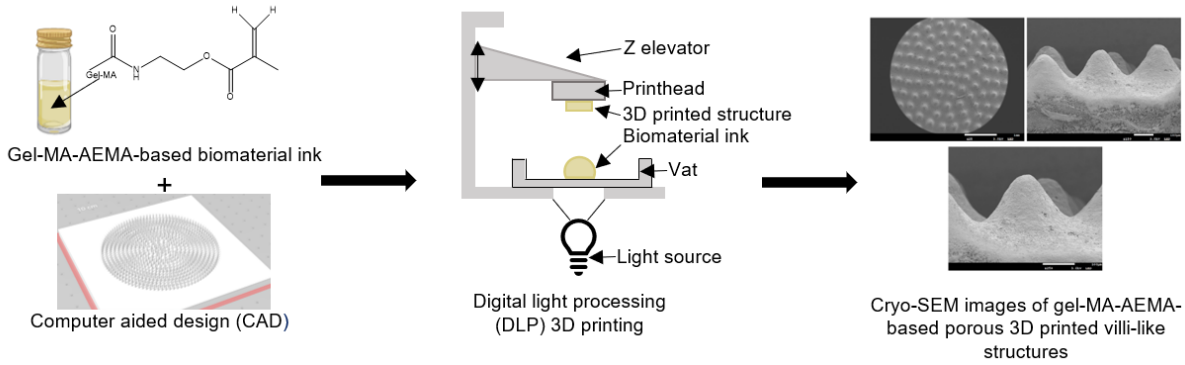

Figure 4. Schematic figure of digital light processing-based 3D printing. First, the biomaterial ink composition was adjusted to the properties of the 3D printer, in combination with a physiologically relevant CAD design. Upon development of the biomaterial ink, a 3D intestine-like hydrogel construct was created, of which the average obtained villi-like structure height is 178±7 µm, while the average thickness is 202±11 µm.

3.2. Assessment of biocompatibility of gel-MA-AEMA-based 3D hydrogel constructs

3.2.1.Cell growth evaluation

The use of 60,000 cells/cm² did not result in a confluent cell monolayer, even after 3 weeks of culture (Figure 5/A), as previously observed when RTdi-MI cells were cultured on Transwell® inserts[7]. By increasing the seeding density to 120,000 – 240,000 cell/cm^2, cell confluency was 80-85% after 24 days of culture. However, to obtain a fully confluent layer, it was necessary to apply a seeding density exceeding 500,000 cells/cm² (500,000 and 900,000 cells/cm²) on the 3D gel-MA-AEMA hydrogel membranes (Figure 5/A, 5/B and 5/C). These results suggest that the enhanced surface roughness due to the porosity of the scaffolds affected cell growth. However, the cell seeding efficiency remained constant as a function of seeding density (between 25.5±9.4%, for 240,000 cells/cm^2 and 16.7±6.9%, for 900,000 cells/cm^2, see *Analysis of seeding efficiency* in SI, Figure S2). Moreover, seeding at a density of 500,000 and 900,000 cells/cm^2 induced the formation of a confluent cell layer within 3 days of cell culture demonstrating the biocompatibility of the hydrogel.

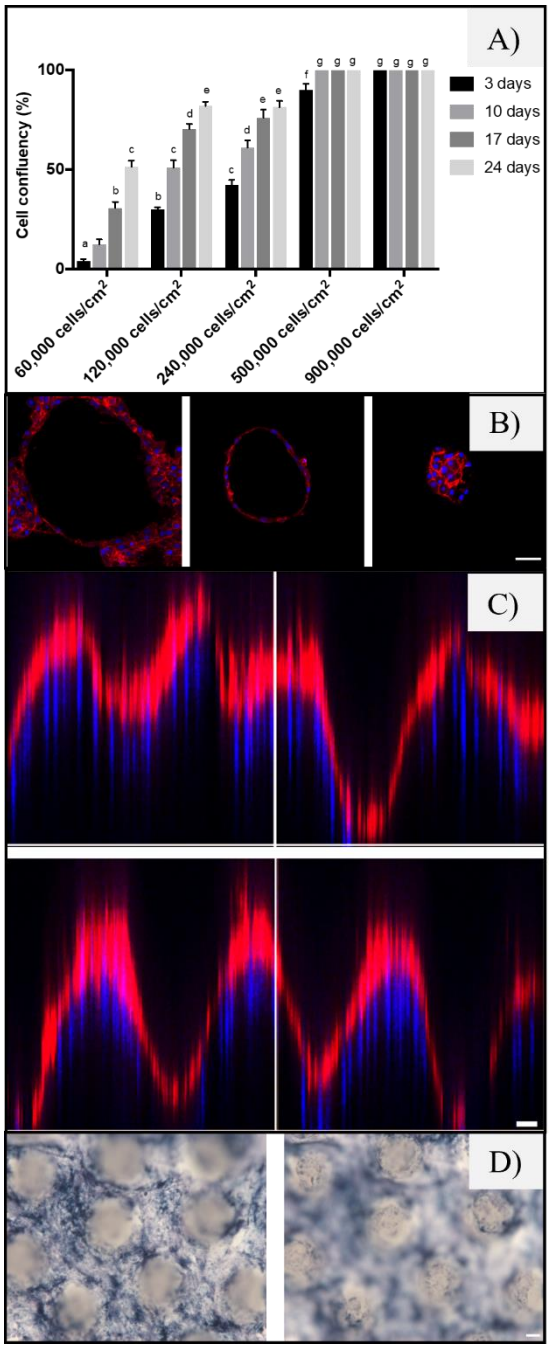

Figure 5. Biocompatibility assays of the 3D gel-MA-AEMA hydrogel membranes cultured with Rainbow Trout (RT) intestinal epithelial cells. Figure 5/A Percentage of confluency (%) of cells seeded at different densities and cultured during 24 days. Figure 5/B Representative picture of RT cells grown on the villi-like shape of the 3D hydrogels. The image shows the cytoskeleton (F-actin, red) and nuclei (DAPI, blue) staining of the cells at the base (left picture), medium height (center picture) and apex (right picture) of the villi-like shape. Scale bar = 50 µm B) Figure 5/C Representative picture of xy and xz views of RT cells grown on 3D hydrogels. Scale bars = 50 µm. Figure 5/D Brightfield image of staining for alkaline

phosphatase activity (blue) of RT cells grown on 3D hydrogels at the base (left picture) and at the villi-like shape apex (right picture). Scale bars = 50 µm.

3.2.2.Morphological evaluation

The staining of cell nuclei (with DAPI) and of filamentous actin (with Phalloidin-iFluor 594), a component of the cytoskeleton important in cell mechanical support and movement[44,45] showed that RTdi-MI cells homogeneously grew on the 3D gel-MA-AEMA hydrogel membranes (Figure 5/B and 5/C). Moreover, full coverage of the scaffold surface was realized. Not only the base of the hydrogel was fully confluent (Figure 5/B and 5/C), but also the middle and the top of the villi-like shape (Figure 5/B) were covered by a monolayer of RTdi-MI cells, demonstrating that this scaffold is biocompatible.

3.2.3.Cell differentiation

Alkaline phosphatase activity was used as evidence of cell differentiation towards functional enterocytes as previously described by Pasquariello et al[7] . As shown, the enzymatic activity was detected at the base and at the apex of the villi-like shape of the 3D hydrogel membranes (Figure 5/D). These results demonstrate that the scaffold stimulated the RTdi-MI intestinal epithelial cells to shift towards more differentiated cell phenotypes, since this enzyme has an important role in preserving gut mucosal defense[46,47] and has been used to identify terminally differentiated functional enterocytes[1].

4. Conclusion

This paper describes the formulation of gel-MA-AEMA towards a novel biomaterial ink for digital light processing-based 3D printing. To enhance the permeability properties of the developed biomaterial ink formulation, Tween®20 was successfully utilized as a porogen, which led to a porous hydrogel structure, promoting the diffusion of medium size marker molecules. The biomaterial ink formulation was successfully applied in DLP 3D printing, which resulted in a close mimicry to the native Rainbow Trout distal intestinal (RT-di) morphology. Finally, the combination of the porous, 3D printed,

physiologically relevant scaffolds and RT-diMI cells seeded at 500,000 and 900,000 cells/cm² allowed the formation of an intestinal epithelial monolayer differentiated towards functional enterocytes. Our data indicates that this *in vitro* model could be a promising option to be applied in future experiments towards efficient screening of new fishfeed formulations.

Supporting Information

Supporting Information is available from the Wiley Online Library or from the author.

Acknowledgements

This research has received funding from the European Union's Horizon 2020 research and innovation program under grant agreement No 828835. We would also like to thank the Hercules Foundation for its financial support in the acquisition of the scanning electron microscope JEOL JSM-7100F equipped with the cryo-transfer system Quorum PP3010T (grant no. AUGE-09-029) used in this research. The authors are thankful for the work of Elise Demuynck in the framework of her master thesis and Florian Vanlauwe M.D., for his help with the fluorimetric analysis of the permeability assay.

Received: ((will be filled in by the editorial staff))
Revised: ((will be filled in by the editorial staff))
Published online: ((will be filled in by the editorial staff))

References

[1] N. Verdile, R. Pasquariello, M. Scolari, G. Scir, T. A. L. Brevini, F. Gandolfi, **2020**.

[2] W. Kong, S. Huang, Z. Yang, F. Shi, Y. Feng, Z. Khatoon, *Sci Rep* **2020**, *10*, DOI 10.1038/s41598-019-57063-w.

[3] N. Verdile, G. Cardinaletti, F. Faccenda, T. A. L. Brevini, F. Gandolfi, E. Tibaldi, *Aquaculture* **2022**, 739031.

[4] F. Gandolfi, "Fish-AI," can be found under http://fish-ai.eu/, **2019**.

[5] J. Wang, P. Lei, A. A. A. Gamil, L. Lagos, Y. Yue, K. Schirmer, L. T. Mydland, M. Øverland, Å. Krogdahl, T. M. Kortner, *Front Immunol* **2019**, *10*, DOI 10.3389/fimmu.2019.00152.

[6] S. S. Crawford, A. M. Muir, *Rev Fish Biol Fish* **2008**, *18*, 313.

[7] R. Pasquariello, N. Verdile, R. Pavlovic, S. Panseri, K. Schirmer, T. A. L. Brevini, F. Gandolfi, *Cells* **2021**, *10*, DOI 10.3390/cells10061555.

[8] A. Kawano, C. Haiduk, K. Schirmer, R. Hanner, L. E. J. Lee, B. Dixon, N. C. Bols, *Aquac Nutr* **2011**, *17*, DOI 10.1111/j.1365-2095.2010.00757.x.

[9] N. Verdile, R. Pasquariello, T. A. L. Brevini, **2020**.

[10] P. Fratzl, F. G. Barth, *Nature* **2009**, *462*, 442.

[11] A. Buxboim, I. L. Ivanovska, D. E. Discher, *J Cell Sci* **2010**, *123*, 297.

[12] M. Tatullo, M. Marrelli, G. Falisi, C. Rastelli, F. Palmieri, M. Gargari, B. Zavan, F. Paduano, V. Benagiano, *Int J Immunopathol Pharmacol* **2016**, *29*, 3.

[13] P. Deptuła, D. Łysik, K. Pogoda, M. Cieśluk, A. Namiot, J. Mystkowska, G. Król, S. Głuszek, P. A. Janmey, R. Bucki, *ACS Biomater Sci Eng* **2020**, *6*, 5620.

[14] G. A. Kim, J. R. Spence, S. Takayama, *Curr Opin Biotechnol* **2017**, *47*, 51.

[15] S. Maji, H. Lee, *Int J Mol Sci* **2022**, *23*, DOI 10.3390/ijms23052662.

[16] C. F. Guimarães, L. Gasperini, A. P. Marques, R. L. Reis, *Nat Rev Mater* **2020**, *5*, 351.

[17] S. S. Soofi, J. A. Last, S. J. Liliensiek, P. F. Nealey, C. J. Murphy, *J Struct Biol* **2009**, *167*, 216.

[18] E. A. Aisenbrey, W. L. Murphy, *Nat Rev Mater* **2020**, *5*, 539.

[19] C. S. Hughes, L. M. Postovit, G. A. Lajoie, *Proteomics* **2010**, *10*, 1886.

[20] J. Creff, L. Malaquin, A. Besson, *J Tissue Eng* **2021**, *12*, DOI 10.1177/2041731420985202.

[21] J. Creff, R. Courson, T. Mangeat, J. Foncy, S. Souleille, C. Thibault, A. Besson, L. Malaquin, *Biomaterials* **2019**, *221*, DOI 10.1016/j.biomaterials.2019.119404.

[22] R. J. Mondschein, A. Kanitkar, C. B. Williams, S. S. Verbridge, T. E. Long, *Biomaterials* **2017**, *140*, 170.

[23] M. Markovic, J. van Hoorick, K. Hölzl, M. Tromayer, P. Gruber, S. Nürnberger, P. Dubruel, S. van Vlierberghe, R. Liska, A. Ovsianikov, *J Nanotechnol Eng Med* **2015**, *6*, DOI 10.1115/1.4031466.

[24] J. Gong, Y. Qian, K. Lu, Z. Zhu, L. Siow, C. Zhang, S. Zhou, T. Gu, J. Yin, M. Yu, H. Wang, H. Yang, *Biomedical Materials (Bristol)* **2022**, *17*, DOI 10.1088/1748-605X/ac96ba.

[25] H. Li, J. Dai, Z. Wang, H. Zheng, W. Li, M. Wang, F. Cheng, *Aggregate* **2022**, DOI 10.1002/agt2.270.

[26] Q. Ge, B. Jian, H. Li, *Forces in Mechanics* **2022**, *6*, DOI 10.1016/j.finmec.2022.100074.

[27] B. Grigoryan, S. J. Paulsen, D. C. Corbett, D. W. Sazer, C. L. Fortin, A. J. Zaita, P. T. Greenfield, N. J. Calafat, J. P. Gounley, A. H. Ta, F. Johansson, A. Randles, J. E. Rosenkrantz, J. D. Louis-Rosenberg, P. A. Galie, K. R. Stevens, J. S. Miller, *Science (1979)* **2019**, *364*, 458.

[28] J. Creff, R. Courson, T. Mangeat, J. Foncy, S. Souleille, C. Thibault, A. Besson, L. Malaquin, *Biomaterials* **2019**, *221*, DOI 10.1016/j.biomaterials.2019.119404.

[29] J. van Hoorick, L. Tytgat, A. Dobos, H. Ottevaere, J. van Erps, H. Thienpont, A. Ovsianikov, P. Dubruel, S. van Vlierberghe, *Acta Biomater* **2019**, *97*, 46.

[30] L. Elomaa, E. Keshi, I. M. Sauer, M. Weinhart, *Materials Science and Engineering C* **2020**, *112*, DOI 10.1016/j.msec.2020.110958.

[31] J. van Hoorick, P. Gruber, M. Markovic, M. Tromayer, J. van Erps, H. Thienpont, R. Liska, A. Ovsianikov, P. Dubruel, S. van Vlierberghe, *Biomacromolecules* **2017**, *18*, 3260.

[32] K. J. de France, F. Xu, T. Hoare, *Adv Healthc Mater* **2018**, *7*, DOI 10.1002/adhm.201700927.

[33] J. Texter, *Colloid Polym Sci* **2009**, *287*, 313.

[34] H. Pan, D. Fan, Z. Duan, C. Zhu, R. Fu, X. Li, *Materials Science and Engineering C* **2019**, *105*, DOI 10.1016/j.msec.2019.110118.

[35] I. Cooperstein, M. Layani, S. Magdassi, *J Mater Chem C Mater* **2015**, *3*, 2040.

[36] M. Markovic, J. van Hoorick, K. Hölzl, M. Tromayer, P. Gruber, S. Nürnberger, P. Dubruel, S. van Vlierberghe, R. Liska, A. Ovsianikov, *J Nanotechnol Eng Med* **2015**, *6*, DOI 10.1115/1.4031466.

[37] N. Verdile, A. Szabó, R. Pasquariello, T. A. L. Brevini, S. van Vlierberghe, F. Gandolfi, *Preparation of Biological Scaffolds and Primary Intestinal Epithelial Cells to Efficiently 3D Model the Fish Intestinal Mucosa*, **2021**.

[38] I. de Decker, A. Szabó, H. Hoeksema, M. Speeckaert, J. R. Delanghe, P. Blondeel, S. van Vlierberghe, S. Monstrey, K. E. Y. Claes, *Journal of Burn Care & Research* **2022**, DOI 10.1093/jbcr/irac165.

[39] B. Claeys, A. Vervaeck, X. K. D. Hillewaere, S. Possemiers, L. Hansen, T. De Beer, J. P. Remon, C. Vervaet, *European Journal of Pharmaceutics and Biopharmaceutics* **2015**, *90*, 44.

[40] N. Gjorevski, N. Sachs, A. Manfrin, S. Giger, M. E. Bragina, P. Ordóñez-Morán, H. Clevers, M. P. Lutolf, *Nature* **2016**, *539*, 560.

[41] S. He, P. Lei, W. Kang, P. Cheung, T. Xu, M. Mana, C. Young Park, H. Wang, S. Imada, J. O. Russell, J. Wang, R. Wang, Z. Zhou, K. Chetal, E. Stas, V. Mohad, M. Halasi, P. Bruun-Rasmussen, I. Adini, R. A. Hodin, Y. Zhang, D. T. Breault, Ö. H. Yilmaz, J. J. Fredberg, N. Saeidi, **n.d.**, DOI 10.1101/2021.03.15.435410.

[42] A. Vedadghavami, F. Minooei, M. H. Mohammadi, S. Khetani, A. Rezaei Kolahchi, S. Mashayekhan, A. Sanati-Nezhad, *Acta Biomater* **2017**, *62*, 42.

[43] N. Torras, J. Zabalo, E. Abril, A. Carré, M. García-Díaz, E. Martínez, **n.d.**, DOI 10.1101/2022.02.09.479715.

[44] T. D. Pollard, J. A. Cooper, *Science (1979)* **2009**, *326*, 1208.

[45] T. Hohmann, F. Dehghani, *Cells* **2019**, *8*, DOI 10.3390/cells8040362.

[46] R. F. Goldberg, W. G. Austen, X. Zhang, G. Munene, G. Mostafa, S. Biswas, M. Mccormack, K. R. Eberlin, J. T. Nguyen, H. S. Tatlidede, H. S. Warren, S. Narisawa, J. L. Millá N ‡, R. A. Hodin, *Intestinal Alkaline Phosphatase Is a Gut Mucosal Defense Factor Maintained by Enteral Nutrition*, **2008**.

[47] J. Fawley, D. M. Gourlay, *Journal of Surgical Research* **2016**, *202*, 225.

To mimic the Rainbow trout intestinal mucosa *in vitro*, a novel 3D culture platform is developed to potentially predict the nutritional value of fish feed as a powerful industrial tool. To this end, a gel-MA-AEMA-based, porous hydrogel scaffold is fabricated via DLP 3D printing, followed by the establishment of a functional monolayer of epithelial RTdi-MI cells on the scaffolds.

A. Szabó Author 1, R. Pasquariello Corresponding Author 2, P. F. Costa Author 3, R. Pavlovic Author 4, I. Geurs Author 5, K. Dewettinck Author 6, Chris Vervaet Author 7, T. A. L. Brevini Author 8, F. Gandolfi Author 9, S. Van Vlierberghe Corresponding Author 10

Light-based 3D printing of gelatin-based biomaterial inks to create a physiologically relevant *in vitro* fish intestinal model